INL/CON-08-14038
PREPRINT

Challenges in Generating Hydrogen by High Temperature Electrolysis Using Solid Oxide Cells

NHA 08

M. S. Sohal
J. E. O'Brien
C. M. Stoots
M. G. McKellar
E. A. Harvego
J. S. Herring

March 2008

The INL is a
U.S. Department of Energy
National Laboratory
operated by
Battelle Energy Alliance

Idaho National Laboratory

CHALLENGES IN GENERATING HYDROGEN BY HIGH TEMPERATURE ELECTROLYSIS USING SOLID OXIDE CELLS

M. S. Sohal, J. E. O'Brien, , C. M. Stoots, M. G. McKellar, E. A. Harvego, J. S. Herring
Idaho National Laboratory, Idaho Falls, ID 83415-3815
Manohar.sohal@inl.gov

Abstract

Idaho National Laboratory's (INL) high temperature electrolysis (HTE) research to generate hydrogen using solid oxide electrolysis cells is presented in this paper. The research results reported here have been obtained in a laboratory-scale apparatus. These results and common scale-up issues also indicate that for the technology to be successful in a large industrial setting, several technical, economical, and manufacturing issues have to be resolved. Some of the issues related to solid oxide cells include stack design and performance optimization, identification and evaluation of cell performance degradation parameters and processes, integrity and reliability of the solid oxide electrolysis (SOEC) stacks, life-time prediction and extension of the SOEC stack, and cost reduction and economic manufacturing of the SOEC stacks. Besides the solid oxide cells, the balance of the hydrogen generating plant also needs significant development. Plant issues include process heat source needed for maintaining the reaction temperature (~830°C), high temperature heat exchangers and recuperators, equal flow distribution of the reactants into each cell, system analysis of hydrogen and associated energy generating plant, and cost optimization.

An economic analysis of a reference HTE plant was performed using the standardized H2A Analysis Methodology developed by the Department of Energy (DOE) Hydrogen Program, and using realistic financial and cost estimating assumptions. The results of the economic analysis demonstrated that the HTE hydrogen production plant driven by a high-temperature helium-cooled nuclear power plant can deliver hydrogen at a cost of $3.23/kg of hydrogen, assuming an internal rate of return of 10%.

These issues need an interdisciplinary research effort involving federal laboratories, solid oxide cell manufacturers, hydrogen consumers, and other such stakeholders. This paper discusses research and development accomplished by INL on such issues and highlights associated challenges that need to be addressed for hydrogen to become an economical and viable option.

1. Introduction

At present, hydrogen is in demand for the production of fertilizers, upgrading of low-quality crude oils, and the removal of sulfur to meet increasingly stringent environmental requirements. For processing the poorer grades of crude oil and the

Athabasca oil sands, the demand for hydrogen in the petroleum industry will grow significantly. It is possible that eventually hydrogen may become a major transportation - fuel through the use of fuel cells in automobiles. The amount of hydrogen needed for processing a barrel of various forms of oil crudes is: 1-2 kg of H_2 for average crude oil; 2-3 kg of H_2 for heavy crude oil; and 3-5 kg of H_2 for the oil sands. Today, 95% of hydrogen is produced through steam reforming of natural gas. Both the increasing price of natural gas and the need to reduce CO_2 emissions will promote nuclear production of hydrogen. One possible option is to produce hydrogen from either electrolytic or thermochemical processes using process heat and electricity from advanced high-temperature (~850°C) nuclear reactors, which are currently under development. The high temperature electrolytic process has the potential to produce hydrogen with overall system efficiencies near those of the thermochemical processes (45-55%), but without the corrosive conditions of thermochemical processes and without the fossil fuel consumption and greenhouse gas emissions associated with hydrocarbon processes [1-3]. A research project is under way at the Idaho National Laboratory (INL) to simultaneously address related issues to make this technology technically and economically viable. The research project consists of mainly four components: (1) experimental tests aimed at performance characterization of solid oxide electrolysis cells (SOEC) and stacks; (2) three-dimensional computational fluid dynamics (CFD) modeling of high-temperature steam electrolysis in a planar SOEC; (3) process system analysis to evaluate and improve the hydrogen generation efficiencies and economics of coupled hydrogen and nuclear plants; (4) identifying mechanisms responsible for degradation of cell performance and means to increase their longevity. While the first three activities are steadily progressing, the fourth activity is in the initial planning stage.

2. Experimental Testing and Development

The purpose of the experiments is to demonstrate the feasibility of the proposed concept, scale-up the electrolyzer system in manageable steps, and examine the degradation and longevity of the cells. These tests have increased in scale from single button cells through 10 and 25 cell single stacks, and most recently to the testing of a four-stack module (each stack containing 60 cells). Single button cell tests are useful for basic performance characterization of electrode and electrolyte materials and of different cell designs (e.g., electrode-supported, porous metal substrate-supported). The single-cell results demonstrated efficient small-scale hydrogen production, with performance close to theoretical predictions. Results of single-cell and cell stack tests have been documented in several recent papers [4-13].

A general schematic diagram of the test apparatus for the small-scale experiments is shown in Figure 1. Primary system components include gas supply cylinders, gas mass-flow controllers, a humidifier, dew-point measurement stations, temperature and pressure measurement, high-temperature furnace, and a solid oxide electrolysis cell or cell stack. Nitrogen was used as an inert carrier gas. The use of a carrier gas allows for independent variation of both the partial pressures and the flow rates of the steam and hydrogen gases, while continuing to run the experiment at essentially ambient pressure.

The solid oxide cells are fabricated by Ceramatec, Inc. of Salt Lake City, Utah. The internal components of a solid oxide cell are shown in Figure 2. The active surface area per cell is 64 cm^2. It is designed to operate in cross flow, with the steam-hydrogen gas
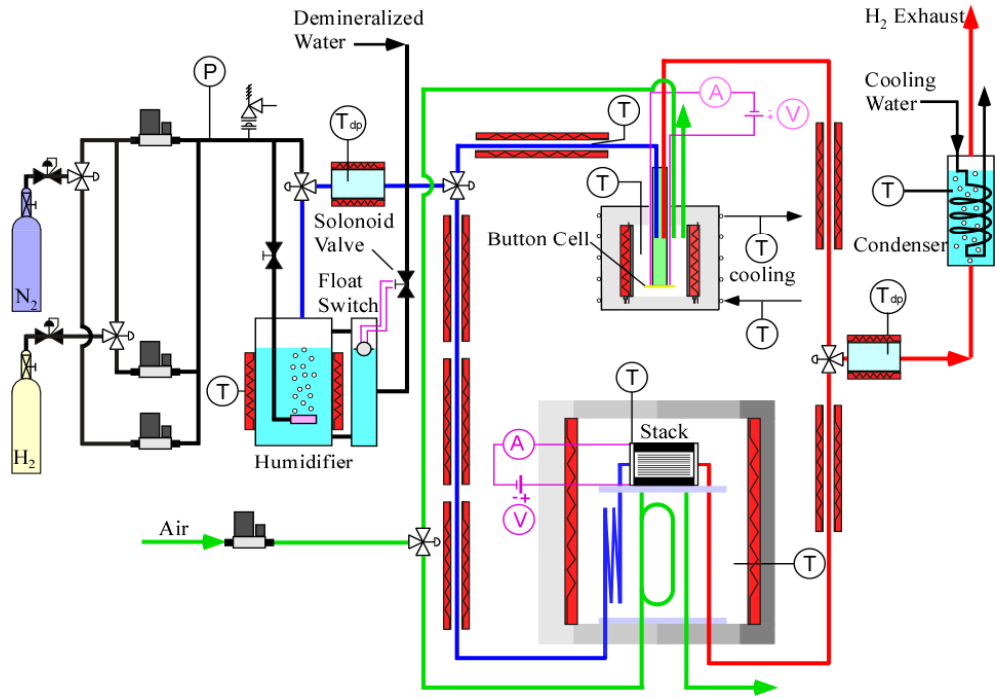
Figure 1. Schematic diagram of apparatus for high temperature electrolysis testing
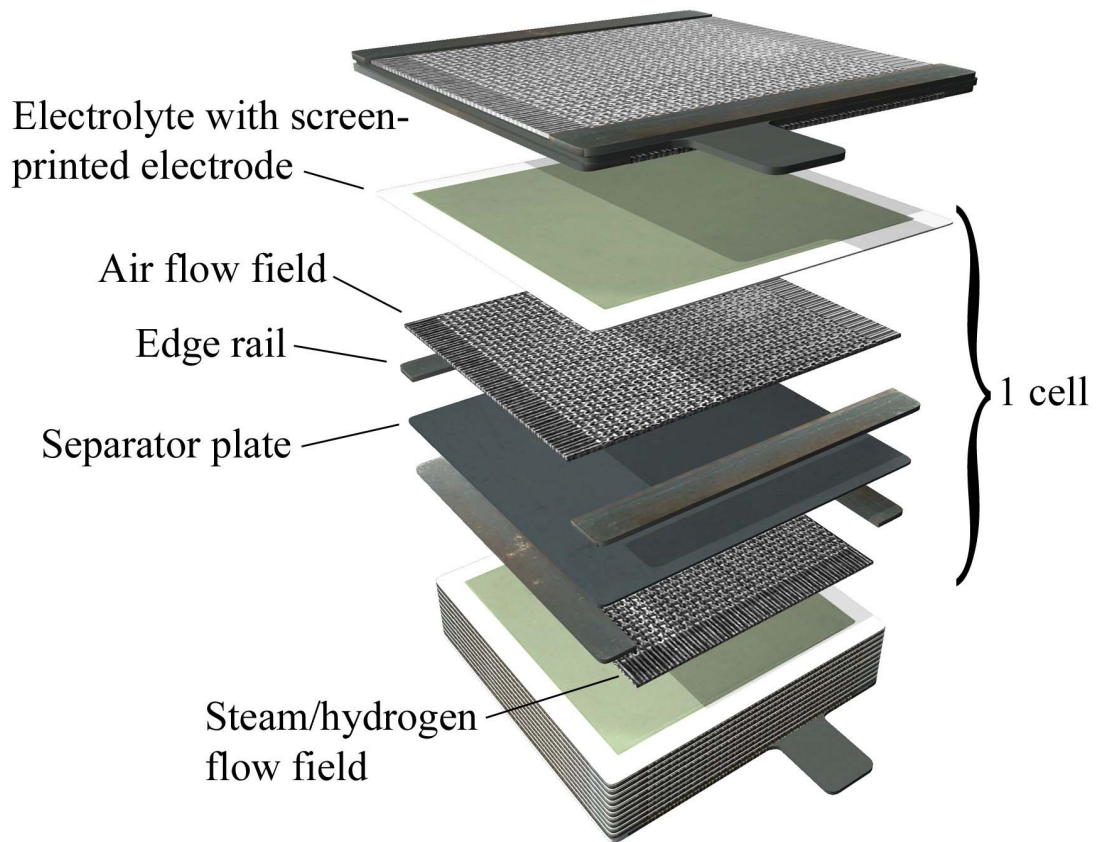

Figure 2. Ceramatec's solid oxide cell/stack construction

mixture entering an inlet manifold on the right (not shown), and exiting through an outlet manifold on the left. Air flow enters at the rear through an air inlet manifold and exits at the front directly into the furnace. The interconnect plate is fabricated primarily from ferritic stainless steel (alloy 441). It includes an impermeable separator plate (~0.46 mm thick) with edge rails and two corrugated "flow fields," one for the air flow and the other for the steam-hydrogen mixture flow, arranged in cross flow. Each flow path includes 32 flow channels across the plate width to distribute gas flow uniformly. The height of the flow channel formed by the edge rails and flow path is 1.02 mm. The steam-hydrogen flow channel is fabricated from nickel. The air-side flow field is ferritic stainless steel. The interconnect plates and flow channels also serve as electrical conductors and current distributors. The electrolyte is scandia-stabilized zirconia, ~140 μm thick. The air-side electrode (anode in the electrolysis mode), is a manganite. The electrode is graded with a manganite zirconia layer (~13 μm) layer on the inside next to the electrolyte and with a pure LSM layer (~18 μm) on the outside. The steam-hydrogen electrode (cathode in the electrolysis mode) is also graded with a nickel-zirconia cermet layer (~13 μm) on the inside in contact with the electrolyte and with a pure nickel layer (~10 μm) on the outside.

The INL is progressing with HTE development per the DOE-Nuclear Hydrogen Initiative plans, progressing from small-scale bench testing to large-scale demonstration with testing at increasing scales and associated development challenges given below:

- Solid oxide electrolysis button cell fabrication and testing (~1 W) - cell material development and performance
- Solid oxide electrolysis stack development and testing (200 W to 5 kW) - electrode and electrolyte materials, interconnect and flow channel materials and fabrication, inter-cell electrical contact, cell and manifold sealing issues, and cell durability
- (Current) Integral laboratory scale (ILS) operation issues (15 kW) - feed-stock heating, high-temperature gas handling, multiple-stack thermal management, heat recuperation, hydrogen recycle
- (Future) Pilot scale facility testing (200/500 kW and 5 MW) - production issues including energy management, utility requirements, high pressure operation, product purification.

Figure 3 shows the progression of the HTE experiments performed at the INL over the past four years, from a 3.2 cm^2 button cell to the present ILS (Figure 4), which will have an active area of 46,080 cm^2 when all three modules are installed. This series of experiments represents a growth in active area and in hydrogen production rate by a factor of ~15,000.

A 25-cell stack was operated continuously in the electrolysis mode for 1000 h. Hydrogen production rates measured during the 1000-h test are presented in Figure 5. The furnace temperature was increased from 800 to 830°C at an elapsed time of 118 h. To measure a cell performance, the area specific resistance (ASR) value of a cell is also calculated. Testing of fuel cells shows that the calculated value of ASR gradually increases over time. It means that the resistance of the cell gradually increases, stack. current decreases, and hydrogen production reduces. Two data sets are shown in Figure 5. The first set shows the hydrogen production rate based on stack current. The second set
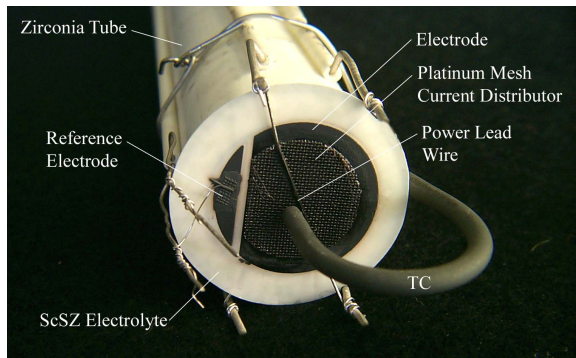
Button Cell (2003), 3.2 cm^2
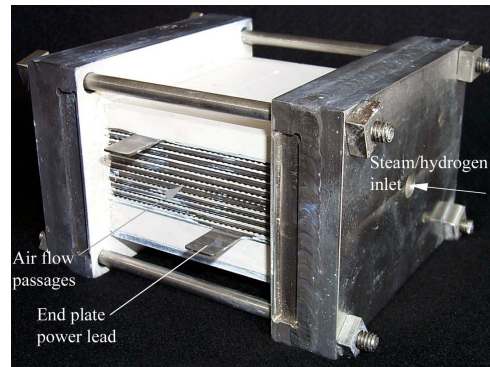
10-cell stack (2004) 640 cm^2

25-cell stack (2005)

240-cell ILS-module (2007) 15,360 cm^2

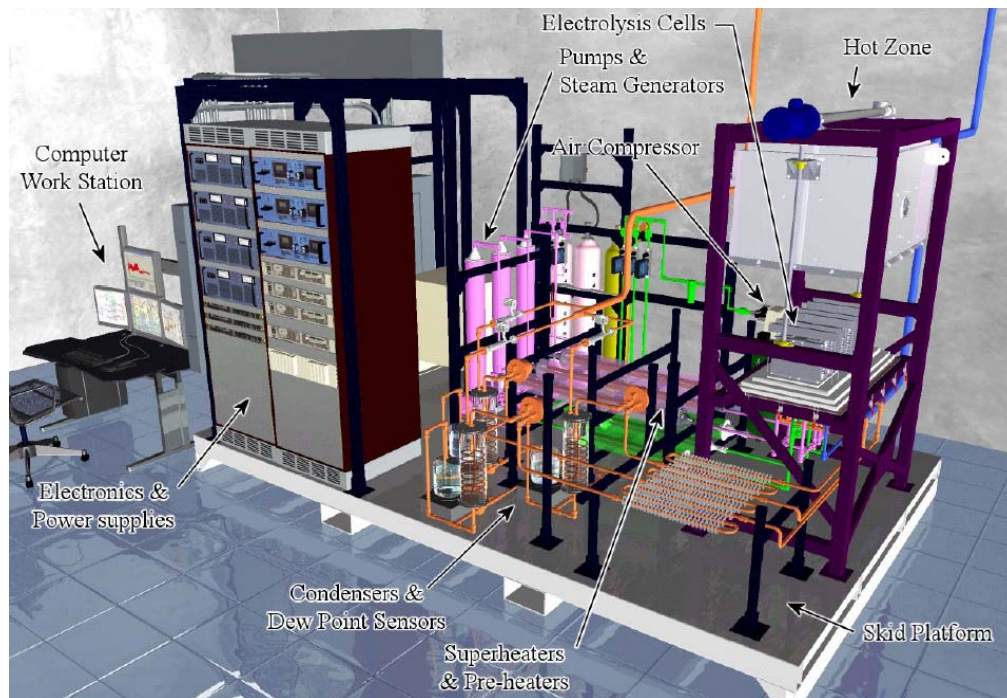Figure 3. Progression and scale-up of high temperature electrolysis testing at INL

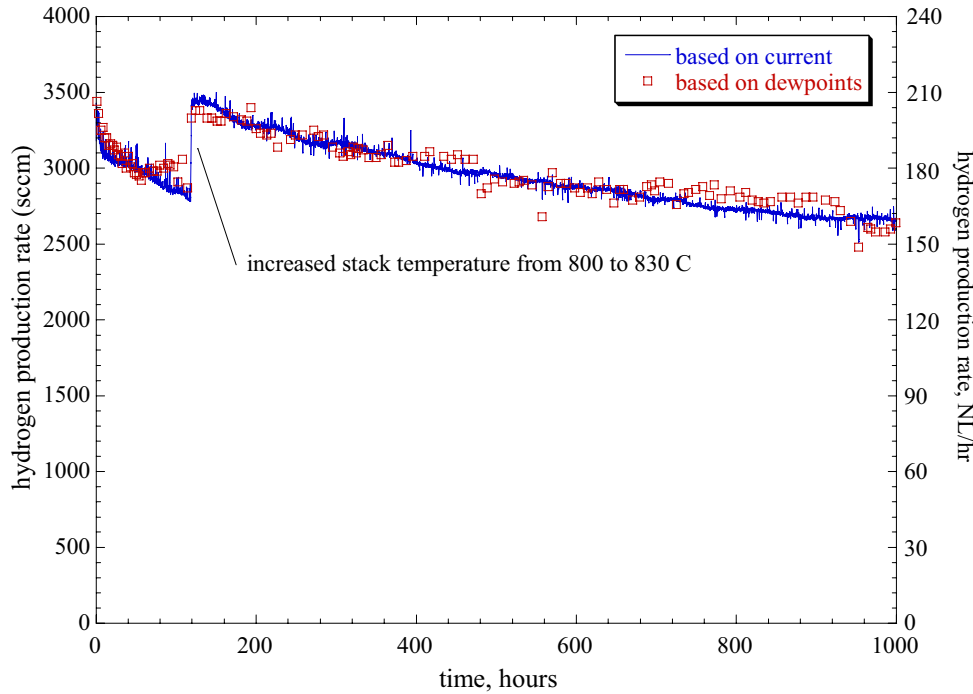Figure 4. Rendering of Integrated Laboratory Scale experimental facility

Figure 5. Hydrogen production rates during 1000-h long-term test.

shows the independent hydrogen production rate based on the measured inlet and outlet dew point temperatures. The figure indicates excellent agreement between two data sets. A significant difference between the two independent hydrogen production rates could indicate a problem such as leakage or a short circuit in the stack. The mean hydrogen production rate during the 1000-h test was 177 NL/h. The slow decrease in hydrogen production is thought to be related primarily to anode degradation, which may lead to higher resistance and lower current. If plotted, the stack current follows the same curve (going down from ~20A to ~17 A) as shown in Figure 5 for hydrogen production rate. The degradation rate decreases with time and is very low for the last 200 h of the test. These experiments have also been effective in examining the performance degradation of solid-oxide cells operating in the steam electrolysis mode for hydrogen production in a temperature range of 800 – 850°C. As the technology of cell fabrication improves, the cell's ability to efficiently produce large quantities or hydrogen over long time-periods should improve.

3. Economic Analysis of a Reference Hydrogen Plant Design

INL has evaluated various concepts for coupling nuclear reactors with high-temperature electrolysis (HTE) hydrogen production plants [14, 15]. A reference design for a commercial-scale HTE plant for hydrogen production was developed to provide a basis for comparing the HTE concept with other hydrogen production concepts and to evaluate relative plant performance economics. The reference plant is powered by a high-temperature helium-cooled nuclear reactor and coupled to a direct Brayton power cycle. The reactor has 600 MWt power, a primary system pressure of 5.0 MPa, and reactor inlet and outlet fluid temperatures of 540°C and 900°C, respectively. The hydrogen generating plant uses 4,009,177 cells, each with a per-cell active area of 225 cm^2. The overall system

thermal-to-hydrogen production efficiency (based on the low heating value of the produced hydrogen) is 47.12% at a hydrogen production rate of 2.356 kg/s. The overall process flow diagram for the high-temperature helium-cooled reactor coupled to the direct helium Brayton power cycle and the HTE plant with air sweep is presented in Figure 5.

The inlet liquid water feedstock at 15.56°C is pressurized to the process pressure of 5.0 MPa. The water stream is then vaporized and pre-heated in the electrolysis recuperator, which recovers heat from the electrolyzer output streams. Downstream of the electrolysis heat recuperator, the steam is mixed with recycled hydrogen product gas to maintain reducing conditions on the steam-hydrogen electrode. The inlet steam-hydrogen (90-10% by volume) mixture is heated in the intermediate heat exchanger (IHX) to the electrolysis operating temperature (~800°C) using high-temperature process heat from the nuclear reactor. The steam-hydrogen mixture then enters the solid oxide electrolysis cell (SOEC) stack, where oxygen is electrolytically removed from the steam, producing hydrogen and oxygen. An additional process heater is also used to add heat from the nuclear reactor primary system to the electrolysis process to maintain the electrolyzer operating conditions at 800°C. Downstream of the electrolyzer, the hydrogen–rich product stream flows through a recuperator where it preheats the inlet process stream of steam-hydrogen. The product stream is further and steam is condensed in the separation tank, yielding dry hydrogen product. The cooled product stream is split and a fraction of the product hydrogen is recycled into the inlet process stream, as discussed previously. The process flow diagram shows air being used as a sweep gas to remove the excess oxygen that is evolved on the anode side of the electrolyzer. The inlet sweep air is compressed to the system operating pressure of 5.0 MPa and is heated from its temperature of ~171°C to the electrolyzer operating temperature of 800°C in the intermediate heat exchanger (IHX) using heat obtained directly from the nuclear reactor. The sweep air then enters the electrolyzer and exits mixed with additional oxygen. Finally, it passes through the electrolysis recuperator to preheat the incoming inlet gas.

Input for the H2A lifecycle cost analysis [16, 17] for the reference HTE design included financial data, and cost information (including capital, operating, maintenance, variable production, and replacement costs). These inputs were based on the several assumptions. Plant-specific financial input by the user includes information on the construction time, plant startup date, plant design production capacity, plant operating capacity factor, capital expenditure rate during construction, and revenue and operating costs during startup using the recommended guidelines of the H2A methodology [16, 17]. The total installed cost of plant equipment was estimated to be $469,159,854, which represents the total depreciable direct capital investment. The total depreciable indirect capital costs (engineering and design, contingencies and licensing/permitting fees) amount to $203,338,738. Adding these costs to the depreciable direct costs, gives a total depreciable capital cost for the reference HTE plant of $672,498,592. The only non-depreciable cost was the cost of land required for the plant site, which is $1,000,000. Adding this cost to the total direct and indirect depreciable capital costs gives a total capital investment cost for the reference HTE plant of $673,498,592. Additional costs to be considered in the reference HTE plant lifecycle analysis are the operation and maintenance (O&M) costs,
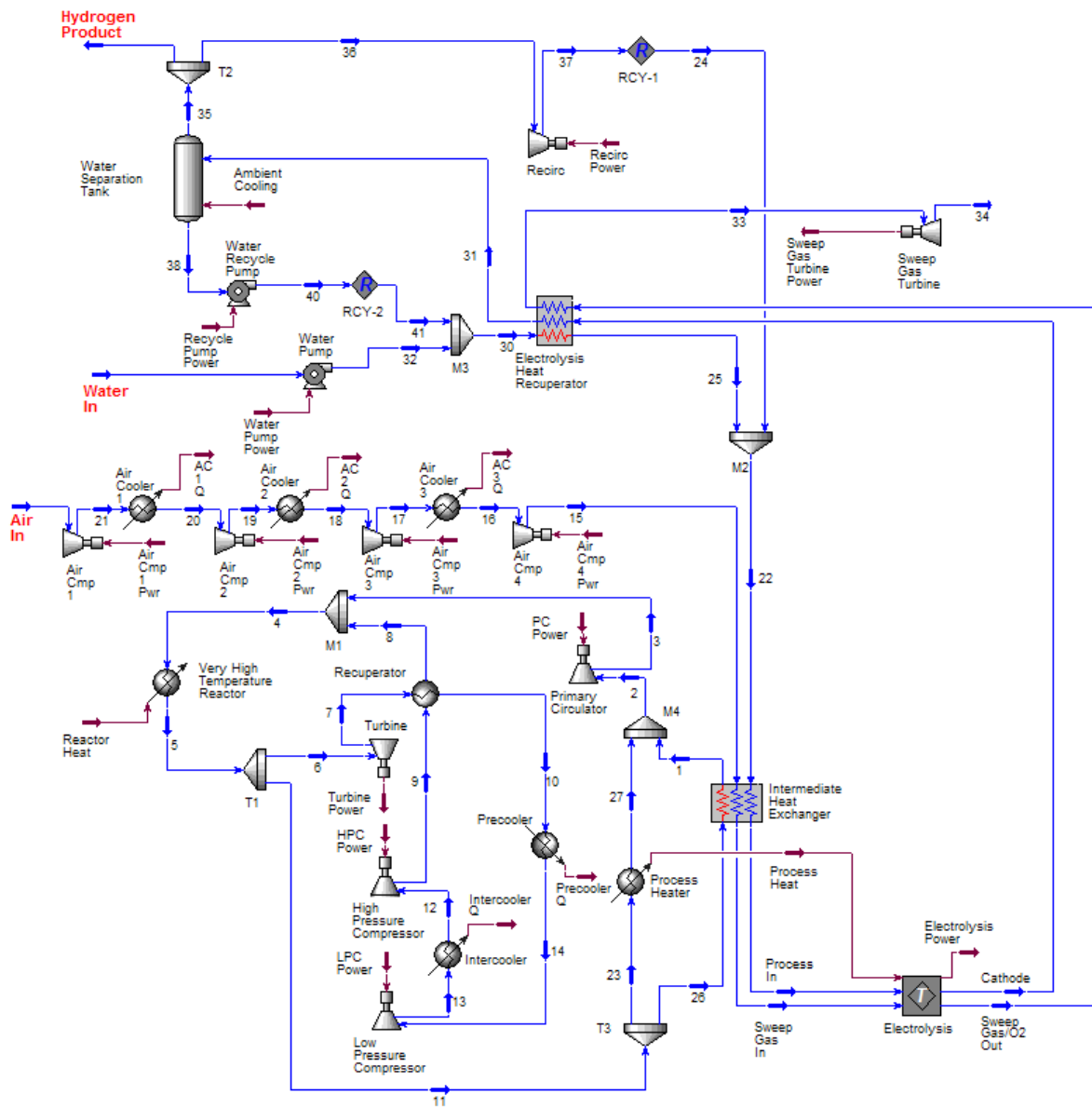
Figure 6. Process flow diagram for helium-cooled reactor/direct Brayton/HTE system with air sweep [16, 17]

which include burdened labor and material costs, various plant permits, licenses, fees and taxes and variable production costs. These total fixed O&M costs amount to $36,827,633/yr. The variable production costs include the cost of the nuclear fuel ($17,800,000 per year) and demineralized water ($790,888), which is the feedstock for the electrolyzer. Adding these variable costs to the fixed O&M costs give a total fixed and variable yearly O&M cost of $55,418,521. The planned replacement costs are the yearly cost of replacement of 1/3 of the Solid Oxide Electrolyzer (SOE) modules, which amounts to $17,186,667/yr. Unplanned replacement costs were assumed to be 2.0% of total depreciable costs per year, and amount to $13,449,972. The financial and cost

information described above provided the input for the H2A lifecycle spreadsheet analysis of the reference HTE hydrogen production plan. Tables 1 and 2 summarize the capital investment and operational cost information developed for the reference HTE plant [18, 19].

Table 1. Summary of capital investment costs (2005 $) [18, 19]

Capital Cost Items	Cost, $
Direct depreciable costs (equipment and systems)	469,159,854
Indirect depreciable costs (site prep., engineering, permitting)	203,338,738
Total direct and indirect depreciable cost	**672,498,592**
Non-depreciable cost (land)	1,000,000
Total capital investment cost	**673,498,592**

Table 2. Summary of operating costs (2005 $) [18, 19]

O&M, Variable and Replacement Cost Items	Cost, $/yr.
Fixed O&M costs (staff, taxes, permitting)	36,827,633
Variable production costs (nuclear fuel and feedwater stock)	18,590,888
Replacement costs (SOE modules and unplanned replacements)	30,636,639
Total yearly costs	**86,055,160**

The results of the H2A lifecycle cost analysis include a cash flow analysis for the plant construction and startup periods, and for the operating life of the plant. The required hydrogen cost (price) in 2005 dollars is also determined based on the plant hydrogen-production capacity and assuming an after-tax internal rate of return of 10%. This reactor outlet temperature, along with the details of the power cycle and electrolyzer yields an overall hydrogen production efficiency of 47.12%. To achieve an after-tax internal rate of return of 10%, the required hydrogen price calculated using the H2A spreadsheet methodology is $3.23/kg. This represents the price or cost of the hydrogen leaving the plant gate at 5 MPa pressure, and does not include any additional storage, delivery, fuel taxes or other costs that the consumer might pay at the pump. As expected, capital costs ($2.36/kg H_2) represent the largest contribution to the total hydrogen cost because of the high construction costs for the nuclear reactor. In this case, nuclear plant capital costs represent about 70% of the total capital cost, or approximately $1.65/kg of hydrogen. The breakdown of these costs showing the different cost contributions is shown in Table 3.

The economic analysis indicates the main cost factors for overall hydrogen generation plant. These being capital cost, power cost, solid oxide cell cost especially if their lifetime is short. It can also provide guidelines to the manufacturers and fabricators of the plant components as to areas for reducing hydrogen cost.

4. CFD Analysis

For detailed SOEC modeling, the commercial CFD code FLUENT was selected. Fluent Inc. developed a solid-oxide fuel cell (SOFC) module for coupling to the core mass, momentum, energy, and species conservation and transport features of the

FLUENT CFD code. The SOFC module models the electrochemical reactions, energy loss mechanisms, and computation of the ionic and electrical flow field throughout the cell. The FLUENT SOFC subroutine was modified for this work to allow for operation in the SOEC mode. Model results provide detailed profiles of temperature, Nernst potential, operating potential, anode-side gas composition, cathode-side gas composition, current density and hydrogen production over a range of stack operating conditions. Results of the numerical model have been compared to experimental results obtained from the SOEC stacks tested at INL [12, 13]. The main advantage of CFD analysis is that its results can reveal abnormal temperature, flow, and electrochemical conditions at any location within a cell. It can point out nonuniform flow, local hot spots, steam starvation, and any such physical and electrochemical condition that may contribute to cell degradation.

Table 3. Hydrogen cost and cost contributions (2005 $) [18, 19]

Hydrogen Cost (Year 2005 \$/kg of H_2)	\$3.229
Capital Cost Contribution (\$/kg of H_2)	\$2.364
Decommissioning Cost Contribution (\$/kg of H_2)	\$0.002
Fixed O&M Cost Contribution (\$/kg of H_2)	\$0.573
Feedstock Cost Contribution (\$/kg of H_2)	\$0.012
Other Raw Material Cost Contribution (\$/kg of H_2)	\$0.000
Byproduct Credit Cost Contribution (\$/kg of H_2)	\$0.000
Other Variable Costs (including utilities) Contribution (\$/kg of H_2)	\$0.278
Total O&M (\$/kg of H_2)	\$0.863

5. Review of Degradation Studies in Solid Oxide Cells

As INL is progressively increasing the scale of electrolyzer systems by increasing the number of solid oxide cells and stacks, it is important to understand and address the causes of performance degradation in solid oxide electrolysis cell (SOEC) stacks. Unfortunately, there are not many studies in the published literature addressing degradation and related issues in SOECs. Even for solid oxide fuel cells (SOFC), the issues of degradation, aging, and longevity are topics of ongoing research. As (thinner) electrolytes with higher ionic conductivity are developed, the overall cell polarization losses are dominated by the electrochemical losses at the anodes and cathodes. Even though the solid oxide cells have several differences while operating in power generating (fuel cell) and electrolysis modes, the degradation mechanisms in the two cases may have some similarities. Therefore, the knowledge of degradation mechanisms in SOFCs can be a starting point for the SOECs and can offer some guidance in identifying the research areas. Because of this reason, some known degradation background in SOFCs is reviewed here.

Ni et al. [30] have developed models for concentration overpotential in SOEC and SOFC as shown in Figure 7a and 7b, respectively. The cathode (hydrogen electrode) in the electrolysis mode is termed as anode in the fuel cell mode. Similarly, the anode (oxygen electrode) in the electrolysis mode is termed as cathode in the fuel cell mode.
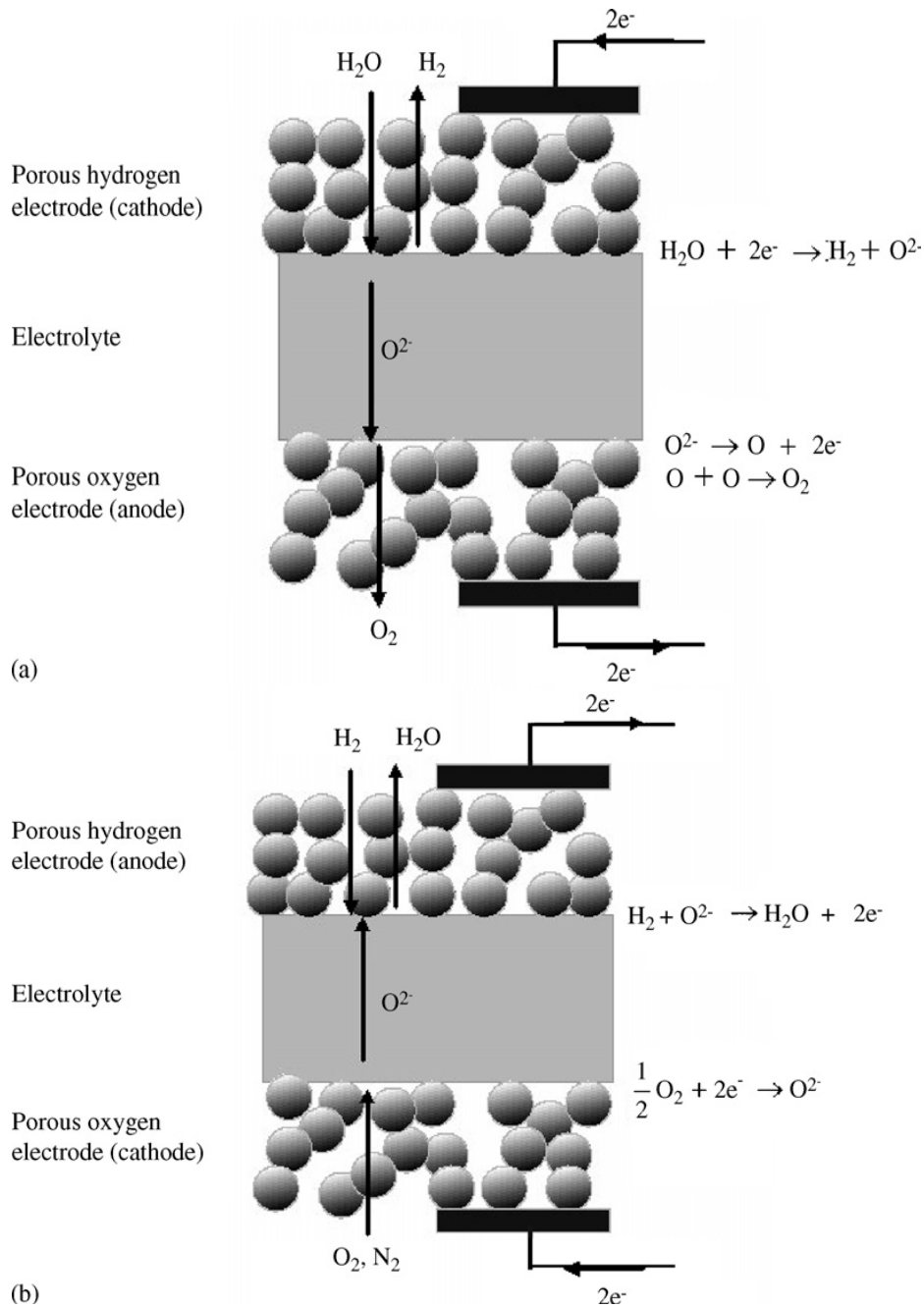
Figure 7. Operating mechanisms of solid oxide cells: (a) SOEC in electrolysis mode, and (b) SOFC in fuel cell mode, Ni et al [30].

Gazzarri and Kesler [20-22] have modeled degradation in solid oxide fuel cells. Under the same operating conditions of temperature and current density, a solid oxide fuel cell (SOFC) and a solid oxide electrolysis cell (SOEC) are likely to have same ohmic and activation overpotentials. During the past few years, extensive research has been performed relating to SOFC. Yet SOFCs have not reached their complete commercial success because of problems relating to their degradation, longevity, and cost. Some of the degradation mechanisms include contact problems between adjacent cell components,

microstructural deterioration (coarsening) of the porous electrodes, and blocking of the reaction sites within the electrodes. Contact problems include delamination of an electrode from the electrolyte, growth of a poorly (electronically) conducting oxide layer between the metallic interconnect plates and the electrodes, and lack of contact between the interconnect and the electrode. Examples of microstructural degradation are anode sintering, carbon deposition, and sulfur or chromium poisoning. Delamination is caused by thermal cycling and it increases ohmic resistance proportional to the delaminated area. Also the delaminated area becomes inactive for electrochemical transport of ions across the electrode and the electrolyte. Chromium-based interconnect oxidation is another important mode that contributes to reducing electrical conductivity between electrode and interconnect. Sometimes ceramic coatings are used to slow down the rate of oxidation and reduce the rate of chromia evaporation from the interconnects. It was also shown that the loss of performance resulting from interconnect detachment is less severe than that caused by electrode delamination because blocked transport of electrons can now easily move laterally in the electrodes as compared to ions being able to move within the electrolyte. Modeling exercise indicated that results of delamination are highly dependent on the inaccuracies in the knowledge of various cell parameters.

Jiang and Chan [23] reviewed performance degradation of an SOFC associated with structural changes in an anode consisting of Ni/yttria-stabilized zirconia (YSZ) during operation. A study by Simwonis et al. [24] exposed a Ni (40 vol%)/8YSZ (60 vol%) cermet anode at 1000°C for 4000 hours in a humidified $Ar/4\%H_2/3\%H_2O$ atmosphere. It was observed that the average Ni particle size increased from 2 to 2.57 μm and the number of Ni particles decreased from 3421 to 2151. The main reason of Ni agglomeration is probably poor wettability characteristics between Ni and YSZ. The agglomeration of Ni particles during SOFC operation results in reduction in electrochemical reaction sites, Ni-to-Ni contacts, and electronic current paths. This phenomenon results in decreasing the electrical conductivity of the anode by 33%. The reduction or prevention of agglomeration and sintering of Ni in the Ni/YSZ cermet electrodes depend strongly on the microstructure of the Ni/YSZ cermet. A detailed and accurate description of the agglomeration and sintering in the Ni/YSZ cermet is rather difficult because of the complex nature of the system. While manufacturing SOFC and SOEC is not an INL objective, understanding a cell's performance in electrolysis mode is.

Tu and Stemming [25] examined the aging mechanisms in anode, cathode, and interconnects in SOFCs. Performance of an SOFC depends on the polarization characteristics of an anode, which depend on the anode morphology. A homogeneous anode consisting of Ni, YSZ, and porosity provide transport paths for electrons, oxide ions, and gases (steam and hydrogen), respectively. Shrinkage of electrode during firing results in lower porosity and decreased gas permeability. One fabrication technique proposed by Itoh [26] is to divide YSZ powder into coarse and fine particles so that during sintering coarse YSZ particles are connected by a network of fine YSZ particles. This kind of microstructure prevents agglomeration and coarsening of Ni particles. Itoh tested a cell with this new design and noted that anodic overpotential remained at ~0.05 V for ~3000 hrs, whereas with older anode design, the anodic overpotential increased to 0.6 V after ~40 hrs of operation.

Jørgensen et al. [27] performed durability tests on an SOFC with cathodes made from strontium-doped lanthanum manganite (LSM) and electrolyte made from YSZ. The tests performed at 1000°C in air for 2000 hrs, but without current load showed little or no degradation. However, the electrodes tested under the same conditions, but with a current density of 300 mA/cm^2 showed ~100% increase in overpotential after 2000 hrs of testing. SEM examination of the electrodes with a current load showed that a large number of ≤1 μm pores were formed on or near the interface between the electrode and the cathode. When ceramic oxide material is exposed to an electric field, local thermodynamics does not remain in equilibrium and the material composition changes locally. When a cation-deficient oxide material is exposed to an oxygen potential gradient, cations can migrate towards higher oxygen potential. The pores are likely to form at the interface with lowest oxygen potential as this part of the interface is unstable. The pores will then move towards the interface with highest oxygen potential. In brief, it appears that sintering properties of cathode layers, the thermodynamic instability of the multicomponent ceramic mixture under operating (ionic and electric) conditions, etc. appear to be the main reasons of increased polarization (overpotential) of the cathodes operating under load.

Recently, Virkar [28] developed an overpotential model for a typical planar SOFC stack comprising of several cells connected in series. He also gave the following argument in favor of developing fundamental understanding of the degradation. In a stack, cell-to-cell characteristics should be as uniform as possible so that at a given operating current, the voltage across each cell is essentially the same. If, because of some structural/fabrication flaws, the cells are not identical, the resistance and voltage drop will vary from cell-to-cell. In such a case, the remainder of the cells in the stack will drive the cell with higher resistance. In an extreme case, for the stack to continue operating, the voltage across a cell with higher resistance can even become negative, which eventually can lead to cell failure and increase in local temperature. This phenomenon can spread to adjacent cells as a domino effect. However, interpretation solely based on visual observations, without a sound theoretical basis for all the phenomena occurring in a cell, may be misleading. In a cell, observations are the aftermath result of some other critical damage to the cell that has already taken place. So the visual observation alone may not be able to show the "root cause" of the problem. Some of the likely reasons of cell degradation include small initial compositional inhomogeneities resulting in large changes in properties, the formation of local hot spots leading to local changes in microstructures and in materials properties, electrode delamination due to thermal cycling/rapid heating, reaction between electrode and electrolyte forming a high resistance layer, fuel and/or oxidant maldistribution, non-uniform oxidation of the interconnect, degradation of the seals, etc. In a normal SOFC, the (oxygen) ionic current is in a direction opposite to that of electronic current. However, if a cell has degraded to cause negative voltage, the direction of electron flow will reverse and both ionic and electronic currents will flow in the same direction. Virkar [28] has developed degradation model based on this premise, that is, a cell with higher resistance compared to the rest of the cells in the stack and operating under a negative voltage will be prone to degradation. Planar stacks are more likely to undergo such a degradation mechanism than tubular stacks. Therefore, the ability to measure voltage across each (planar) cell could help in preventing catastrophic failure by either performing preventive maintenance or shorting

the bad cell. A similar degradation model of an SOEC can also offer some insight into the cell degradation phenomenon during the electrolysis mode.

Yokokawa et al. [29] recently studied the chemical behavior of perovskite cathode/rare earth doped ceria interlayer/YSZ electrolyte multilayer structure and their relation with the cell's performance. To improve the performance of a cell at lower temperatures (~800°C), many changes in cell materials have taken place. However, these changes have also led to several cell degradation problems. These are:

- Metal interconnects give rise to new degradation mechanisms. One is increased resistance across oxide scales on both oxidizing and reducing sides. Another one is cathode degradation (poisoning) caused by chromium oxide vapors, called chromium poisoning.
- Use of thermodynamically less stable materials (La/Sr FeO$_3$, Co/Fe O$_3$) or rare earth doped ceria.
- At lower temperatures, metal carbonates will be formed.
- At lower temperatures, the electrochemical overpotential will increase when the same electrode materials are used.

The overpotentials can be determined by the several models available in the literature, for example, Virkar [28]. However, the concentration overpotentials are different between the SOEC and SOFC modes because of the different gas transport mechanisms in the porous electrodes. Ni et al. [30] showed that concentration overpotentials are the sole factor responsible for the different current–voltage (i - V) characteristics between the SOEC and SOFC modes. Their analytical model shows the difference between the SOEC and SOFC because of difference in gas transport mechanisms in two different modes. The selection of an electrode support can greatly affect the overall performance of a reversible solid oxide cell. A hydrogen-electrode (fuel cell anode) support is favorable to the SOFC mode while an oxygen-electrode (electrolysis anode) support is favorable to the SOEC mode. Therefore, the details of both SOEC and SOFC operating conditions should be carefully considered in their design. If a specified solid oxide cell is mainly used for hydrogen generation, an oxygen-electrode (electrolysis anode) support is recommended.

Mawsdley et al. [31] have presented results of post-test evaluation of the Ceramatec solid oxide cells after a 100-h test in electrolysis mode. They used four-point resistivity measurements, X-ray fluorescence and Raman spectroscopies to study the surface characteristics of cells and bipolar plates. It was concluded that the oxygen electrode has been a major contributor to the cell overpotential. Most of the cell degradation occurred along the edges of the electrodes and at the interfaces.

The above is not a comprehensive review of the degradation mechanisms in a SOFC or SOEC, but an introduction to the ongoing degradation-related research in SOFC, which may offer some guidance as to the work that needs to be done to improve the longevity and performance of SOEC in a hydrogen generating plant. In summary, the main degradation mechanisms as summarized by Blum et al. [32] are listed in Table 4.

Table 4. Main degradation mechanisms in a solid oxide fuel cell, Blum et al. [32]

Components of a solid oxide fuel cell (in a power generation mode)		
Cathode side	**Electrolyte**	**Anode side**
Three phase boundary reduction by: - Cr poisoning - Particle sintering	Phase instabilities Interdiffusion	Ni agglomeration Sulphur poisoning Cracking by reoxidation
Phase change Interdiffusion		Interdiffusion
Contact degradation Resistivity increase Cr transport		Contact loss by - Sintering - Seal swelling - Temperature gradients - Resistivity increase
Interconnect: - Electrical resistance of scales - Cr evaporation - Scale spallation - Inner oxidation - Mechanical distortion		Interconnect: - Electrical resistance of scales - Embrittlement by carburization - Scale spallation - Mechanical distortion

6. Conclusions

Idaho National Laboratory's (INL) high temperature electrolysis research to generate hydrogen using solid oxide electrolysis cells is presented in this paper. The material presented here points to various scale-up and technical issues that need to be addressed for the hydrogen generation technology to be successful on a large industrial scale. Some of these issues are solid oxide stack design, performance optimization, identification and evaluation of cell performance degradation mechanisms and parameters, integrity and reliability of the solid oxide electrolysis (SOEC) stacks, life-time prediction and extension of the SOEC stacks, and economical manufacturing of the SOEC stacks. Some other related issues include identification and optimization of the process and ohmic heat sources needed for maintaining the electrolyzer temperature at ~830°C, intermediate heat exchangers and recuperators, equal distribution of the reactants into each cell, and cost reduction.

An economic analysis of this plant was performed using the standardized H2A Analysis Methodology developed by the Department of Energy (DOE) Hydrogen Program. A high temperature electrolysis hydrogen production plant driven by a high-temperature helium-cooled nuclear power plant can deliver hydrogen at a cost of $3.23/kg of hydrogen assuming an internal rate of return of 10%.

Electrochemical phenomena controlling the degradation mechanisms in solid oxide electrolysis stacks need to be understood. These issues have to be addressed through an interdisciplinary research effort of federal laboratories, solid oxide cell manufacturers, and academic researchers.

Scale-up of the hydrogen generating system, reducing the cost of generating hydrogen, and the life-time extension of the solid oxide cells are three main challenges. These challenges need to be addressed for hydrogen to become an economical and viable option.

References

1. International Atomic Energy Agency (IAEA), Hydrogen as an Energy Carrier and its Production by Nuclear Power, IAEA-TECDOC-1085, May 1999.
2. National Academy of Sciences, National Research Council, The Hydrogen Economy: Opportunities, Costs, Barriers, and R&D Needs, February 2004.
3. B. Yildiz and M. S. Kazimi, "Nuclear Energy Options for Hydrogen and Hydrogen Based Liquid Fuels Production," MIT-NES-TR-001, September 2003.
4. J. E. O'Brien, C. M. Stoots, J. S. Herring, and P. A. Lessing, "Characterization of Solid-Oxide Electrolysis Cells for Hydrogen Production via High-Temperature Steam Electrolysis," Proceedings of Second International Conference on Fuel Cell Science, Engineering, and Technology, Rochester, NY, paper #2474, June 14-16, 2004, pp. 219-228.
5. J. E. O'Brien, C. M. Stoots, J. S. Herring, and P. A. Lessing, J. J. Hartvigsen, S. Elangovan, "Performance Measurements of Solid-Oxide Electrolysis Cells for Hydrogen Production from Nuclear Energy," J. Fuel Cell Scince and Technology, Vol. 2, No. 3, 2005, pp. 156-163.
6. J. S. Herring, J. E. O'Brien, C. M. Stoots, P. A. Lessing, R. P. Anderson, J. J. Hartvigsen, "Hydrogen Production From Nuclear Energy via High-Temperature Electrolysis," International Conference on Advances in Nuclear Power Plants (ICAPP '04), Pittsburgh, PA, June 13–17, 2004.
7. J. S. Herring, J. E. O'Brien, C. M. Stoots, P. A. Lessing, R. P. Anderson, J. J. Hartvigsen, and S. Elangovan, "Hydrogen Production through High-Temperature Electrolysis using Nuclear Power," AIChE Spring National Meeting, New Orleans, LA, April 25–29, 2004.
8. J. E. O'Brien, C. M. Stoots, J. E. Herring, and P. A. Lessing, "Performance Measurements of Solid-Oxide Electrolysis Cells for Hydrogen Production from Nuclear Energy," 12th ICONE Meeting, Arlington, VA, paper # ICONE12-49479, April 25-29, 2004.
9. J. E. O'Brien, C. M. Stoots, S. J. Herring, and J. J. Hartvigsen, "High-Temperature Electrolysis for Hydrogen Production from Nuclear Energy," 11th International Topical Meeting on Nuclear Reactor Thermal-Hydraulics (NURETH-11), Avignon, France, October 2-6, 2005.
10. J. E. O'Brien, C. M. Stoots, J. S. Herring, and J. J. Hartvigsen, "Hydrogen Production Performance of a 10-Cell Planar Solid-Oxide Electrolysis Stack," J. Fuel Cell Science and Technology, Vol. 3, 2006, pp. 213-219.
11. J. E. O'Brien, C. M. Stoots, J. S. Herring, and J. J. Hartvigsen, "High Temperature Electrolysis for Hydrogen Production from Nuclear Energy," Nuclear Technology, Vol. 158, 2007, pp. 118-131.
12. G. L. Hawkes, J. E. O'Brien, C. M. Stoots, J. S. Herring, "CFD Model of a Planar Solid-Oxide Electrolysis Cell for Hydrogen Production from Nuclear Energy," Paper # 326, 11th International Topical Meeting on Nuclear Reactor Thermal-Hydraulics (NURETH-11), Avignon, France, October 2-6, 2005.
13. G. L. Hawkes, J. E. O'Brien, C. M. Stoots, and J. S. Herring, "Computational Fluid Dynamics Model of a Planar Solid-Oxide Electrolysis Cell for Hydrogen Production from Nuclear Energy," Nuclear Technology, Vol. 158, 2007, pp. 132-144.
14. J. E. O'Brien, M. G. McKellar, and J. S. Herring, "Performance Predictions for Commercial-Scale High-Temperature Electrolysis Plants Coupled to Three Advanced Reactor Types," ANS International Congress on Advances in Nuclear Power Plants (ICAPP08), June 8-12, 2008, Anaheim, CA.
15. E. A. Harvego, M. G. McKellar, J. E. O'Brien, and J. S.Herring, "Summary of Reactor-Coupled HTE Modeling Sensitivity Studies," INL Internal Report, October 26, 2006.
16. US DOE Hydrogen Program Website, DOE H2A Analysis, http://www.hydrogen.energy.gov/h2a_analysis.html.
17. U.S. DOE, "H2A Central Hydrogen Production Model Users Guide," Version 1.0.10, July 2005.
18. E. A. Harvego, M. G. McKellar, M. S. Sohal, J. E. O'Brien, J. S. Herring, "Economic Analysis of the Reference Design for a Nuclear-Driven High-Temperature-Electrolysis Hydrogen Production Plant," INL External Report, INL/EXT/-08-13799, January 30, 2008.

19. E. A. Harvego, M. G. McKellar, M. S. Sohal, J. E. O'Brien, J. S. Herring, "Economic Analysis of a Nuclear Reactor Powered High-Temperature-Electrolysis Hydrogen Production Plant," Under publication.
20. J. I. Gazzari and O. Kesler, "Non-destructive Delamination Detection in Solid Oxide Fuel Cells," J. Power Sources, Vol. 167, 2007, pp. 430-441.
21. J. I. Gazzari and O. Kesler, "Short-stack Modeling of Degradation in Solid Oxide Fuel Cells Part I. Contact Degradation," J. Power Sources, Vol. 176, 2008, pp. 138-154.
22. J. I. Gazzari and O. Kesler, "Short-stack Modeling of Degradation in Solid Oxide Fuel Cells Part II. Sensitivity and Interaction Analysis," J. Power Sources, Vol. 176, 2008, pp. 155-166.
23. S. P. Jiang and S. H. Chan, "A Review of Anode Materials Development in Solid Oxide Fuel Cells," J. Materials Science, Vol. 39, 2004, pp. 4405-4439.
24. D. Simwonis, F. Tietz, and D. Stöver, "Nickel Coarsening in Annealed Ni/8YSZ Anode Substrates for Solid Oxide Fuel Cells," Solid State Ionics, Vol. 132, No. 3-4, 2000, pp. 241-251.
25. H. Tu and U. Stemming, "Advances, Aging Mechanisms, and Lifetime in Solid-Oxide Fuel Cells," J. Power Sources, Vol. 127, 2004, pp. 284-293.
26. H. Itoh, "Research and Development on High Performance Anode for Solid-Oxide Fuel Cells – Improvements of the Microstructure for New Long Life Anode," Central Research Institute of Electric Power Industry (CRIEPI) Report W94016, 1995.
27. M. J. Jørgensen, P. Holtappels, and C. C. Appel, "Durability Test of SOFC Cathodes," J. Applied Electrochemistry, Vol. 30, 2000, pp. 411-418.
28. A. V. Virkar, "A Model for Solid Oxide Fuel Cell (SOFC) Stack Degradation," J. Power Sources, Vol. 172, 2007, pp. 713-724.
29. H. Yokokawa, N. Sakai, T. Horita, K. Yamaji, M. E. Brito, and H. Kishimoto, "Thermodynamic and Kinetic Considerations on Degradations in Solid Oxide Fuel Cell Cathodes," J. Alloys and Compounds, Vol. 452, 2008, pp. 41-47.
30. M. Ni, M. K.H. Leung, D. Y. C. Leung, "A modeling study on concentration overpotentials of a reversible solid oxide fuel cell," J. Power Sources, Vol. 163, 2006, pp. 460–466.
31. J. R. Mawdsley, et al., "Post-Test Evaluation of the Oxygen Electrode from a Solid Oxide Electrolysis Stack and Electrode Materials Development," AIChE Meeting, Salt Lake City, UT, November 5-9, 2007.
32. L. Blum et al., "Solid Oxide Fuel Cell Development at Forschungszentrum Juelich," Fuel Cells 07, No. 3, 2007, pp. 204-210.